Binuclear Phosphido-Bridged Tungsten–Rhodium Complexes. Crystal and Molecular Structure of the Dimeric Bimetallic Complex $[(CO)_4W(\mu\text{-}PPh_2)_2Rh(\mu\text{-}CO)]_2$ with a Bent Metal Chain

Peter M. Shulman, Eric D. Burkhardt, Eric G. Lundquist, Robert S. Pilato, and Gregory L. Geoffroy*

Department of Chemistry, The Pennsylvania State University, University Park, Pennsylvania 16802

Arnold L. Rheingold

Department of Chemistry, University of Delaware, Newark, Delaware 19711

Received February 7, 1986

The new phosphido-bridged W–Rh complexes $(CO)_4\overline{W(\mu\text{-}PPh_2)_2}RhH(CO)(PPh_3)$ (**2**), $(CO)_4\overline{W(\mu\text{-}PPh_2)_2}RhH(COD)$ (**3**; COD = 1,5-cyclooctadiene), and $(CO)_4\overline{W(\mu\text{-}PPh_2)_2}Rh(cyclooctenyl)$ (**4**) have been prepared and characterized. Complex **2** has been structurally characterized: $P2_1/n$, a = 11.430 (3) Å, b = 19.085 (5) Å, c = 20.738 (6) Å, β = 100.80 (2)°, V = 4444 (2) Å^3, Z = 4, R = 0.0393, R_w = 0.0420 for 5754 reflections with $F_o > 4\sigma(F_o)$. The two μ-PPh_2 ligands bridge the W–Rh bond with the W further coordinated by four COs and the Rh by hydride, CO, and PPh_3 ligands. Complex **4** reacts with CO to yield the tetrametallic complex $[(CO)_4\overline{W(\mu\text{-}PPh_2)_2}Rh(\mu\text{-}CO)]_2$ (**13**) which has been structurally characterized: $P\bar{1}$, a = 13.580 (2) Å, b = 19.838 (4) Å, c = 22.299 (5) Å, α = 82.94 (2)°, β = 79.17 (2)°, γ = 88.63 (2)°, V = 5857 (2) Å^3, Z = 4, R = 0.0619, R_w = 0.0699 for 6749 reflections with $F_o > 3\sigma(F_o)$. Two crystallographically independent but chemically similar molecules form the asymmetric unit; the two molecules form an enantiomeric pair. The four metal atoms of each molecule are arranged in a bent chain with the W atoms at the end and the Rh atoms in the middle of the chain, and all metal–metal distances are consistent with single metal–metal bonds. The two Rh's are bridged by two carbonyl ligands, and the W–Rh units are each bridged by two μ-PPh_2 ligands. Complex **13** rapidly reacts with $CO/H_2/PPh_3$ to cleave the Rh–Rh bond and form complex **2**. This latter complex was found to readily react with ethylene to transform one of the μ-PPh_2 bridges into a PPh_2Et ligand and give $(CO)_4(PPh_2Et)\overline{W(\mu\text{-}PPh_2)}Rh(CO)(PPh_3)$. Similar bridge elimination occurs when the anionic complex $[(CO)_4\overline{W(\mu\text{-}PPh_2)_2}Rh(CO)(PPh_3)]^-$ is treated with CH_3OTf.

Heterobimetallic complexes offer the promise of unique reactivity as a result of combining metals with inherently different sets of chemical properties.[1] One problem that must be solved in order to fully exploit this potential lies in the relative ease with which many of these fragment when placed under reaction conditions. In our studies we have used the μ-PPh_2 ligand to bridge adjacent metals so as to retard such fragmentation reactions, and these ligands often serve that purpose well. However, μ-PR_2 ligands are not inert as they can participate in reaction chemistry, often in unwanted ways.[2]

The μ-PPh_2 ligand was selected in large part because of the utility of these ligands in directing the syntheses of desired compounds via the "bridge-assisted" synthetic pathway.[1] An illustration is the preparation of the μ-PPh_2 bridged W–Ir complex **1** by the reaction sequence given in eq 1.[3] Compound **1** gave rise to an interesting series

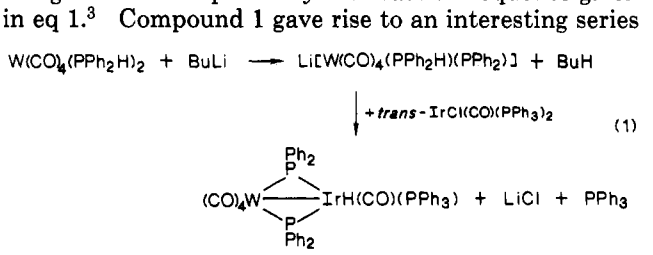

1

of binuclear acyl–hydride and carbene–hydride derivatives, but it showed no examples of unusual bimetallic reactivity.[3] This we believe is in part due to the inertness of the Ir(3+) center in this complex.

We have sought to increase the reactivity of the above class of compounds by two strategies. In work to be reported elsewhere,[4] the CO and PPh_3 ligands on the Ir center have been replaced by a 1,5-cyclooctadiene (COD) ligand. The latter has the potential to yield open coordination sites on Ir by hydrogen transfer to the olefin ligand. In the present study, we have chosen to replace Ir by the more reactive metal Rh, as well as incorporate a COD ligand. Herein is described the preparation of new bimetallic W–Rh complexes **2**, **3**, and **4**.

Complex **2** is particularly interesting since the coordination environment of the Rh end of the molecule resembles $RhH(CO)(PPh_3)_3$, a well-known hydroformylation

(1) Roberts, D. A.; Geoffroy, G. L. In *Comprehensive Organometallic Chemistry*; Wilkinson, G., Stone, F. G. A., Abel, E. W., Eds.; Pergamon: Oxford, 1982; Chapter 40.

(2) (a) Geoffroy, G. L.; Rosenberg, S.; Shulman, P. M.; Whittle, R. R. *J. Am. Chem. Soc.* **1984**, *106*, 1519. (b) Harley, A. D.; Guskey, G. J.; Geoffroy, G. L. *Organometallics* **1983**, *2*, 53. (c) Burkhardt, E. W.; Mercer, W. C.; Geoffroy, G. L.; Rheingold, A. L.; Fultz, W. C. *J. Chem. Soc., Chem. Commun.* **1983**, 1251. (d) Rosenberg, S.; Whittle, R. R.; Geoffroy, G. L. *J. Am. Chem. Soc.* **1984**, *106*, 5934. (e) Klingert, B.; Werner, H. *J. Organomet. Chem.* **1983**, *252*, C47. (f) Werner, H.; Zolk, R. *Organometallics* **1985**, *4*, 601. (g) Maclaughlin, S. A.; Carty, A. J.; Taylor, N. J. *Can. J. Chem.* **1982**, *60*, 87. (h) Patel, V. D.; Taylor, N. J.; Carty, A. J. *J. Chem. Soc., Chem. Commun.* **1984**, 99. (i) Smith, W. F.; Taylor, N. J.; Carty, A. J. *J. Chem. Soc., Chem. Commun.* **1976**, 896. (j) Regragui, R.; Dixneuf, P. H.; Taylor, N. J.; Carty, A. J. *Organometallics* **1984**, *3*, 814. (k) Seyferth, D.; Wood, T. G.; Fackler, J. P., Jr.; Mazany, A. M. *Organometallics* **1984**, *3*, 1121. (l) Henrick, K.; Iggo, J. A.; Mays, M. J.; Raithby, P. R. *J. Chem. Soc., Chem. Commun.* **1984**, 209. (m) Yu, Y.-F.; Chau, C.-N.; Wojcicki, A.; Calligaris, M.; Nardin, G.; Balducci, G. *J. Am. Chem. Soc.* **1984**, *106*, 3704. (n) Shyu, S.-G.; Wojcicki, A. *Organometallics* **1984**, *3*, 809. (o) Yu, Y.-F.; Gallucci, J.; Wojcicki, A. *J. Am. Chem. Soc.* **1983**, *105*, 4826.

(3) Breen, M. J.; Shulman, P. M.; Geoffroy, G. L.; Rheingold, A. L.; Fultz, W. C. *Organometallics* **1984**, *3*, 782.

(4) Rosenberg, S.; Mahoney, W. S.; Hayes, J. M.; Geoffroy, G. L.; Rheingold, A. L. *Organometallics* **1986**, *5*, 1065.

0276-7333/87/2306-0101$01.50/0

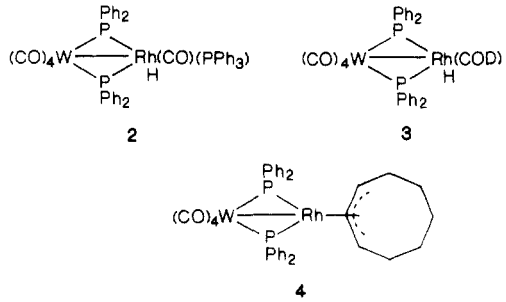

2 3 4

catalyst.[5] Thus, if such a complex were to show catalytic activity, it would be interesting to explore the effect of the adjacent metal W on its catalytic properties. However, as described herein and previously communicated,[2a] complex **2** is not a suitable catalyst since it readily undergoes a bridge-elimination reaction in the presence of olefins. From complex **4**, a new tetrametallic W_2Rh_2 complex with a bent metal chain has been prepared and structurally characterized, and those results are also described herein.

Results and Discussion

Syntheses. The new complexes were prepared by using the bridge-assisted method[1] beginning with the phosphidometalates **5** and **6** prepared in situ by the reactions of eq 2. From these, the anionic complexes **7** and **8** were

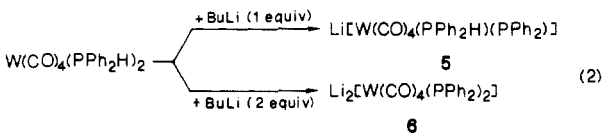

(2)

obtained by reactions 3 and 4. These anionic complexes

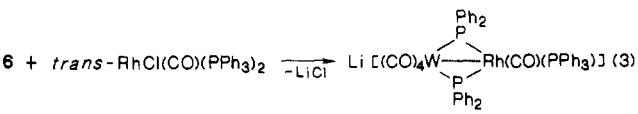

(3)

7

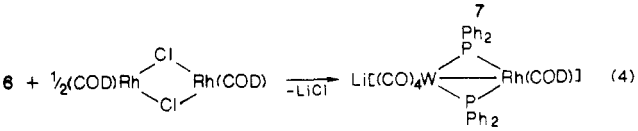

(4)

8

have proven too unstable to isolate in pure form, but their conversions to the well-characterized complexes described below and the spectroscopic data for **7** leave little doubt as to their formulations. Spectroscopic data for all the new complexes prepared in this study are given in the Experimental Section with ^{31}P NMR data listed in Table I. At −61 °C, the ^{31}P NMR spectrum of **7** shows a doublet at δ 202.9 ($J_{P\text{-}Rh}$ = 139.2 Hz) due to equivalent μ-PPh_2 ligands and a second doublet at δ 45.3 ($J_{P\text{-}Rh}$ = 189.9 Hz) assigned to the Rh–PPh_3 ligand. The downfield position of the μ-PPh_2 resonance implies the presence of a W–Rh bond in **7**,[6] and the absence of ^{31}P–^{31}P coupling indicates a tetrahedral ligand arrangement about Rh.[7] Upon warming to room temperature, the ^{31}P NMR spectrum broadens, but the resonances still show ^{103}Rh–^{31}P coupling and do not shift in position. While the reasons for this broadening

Table I. ^{31}P NMR Data in C_6D_6 Solution

complex	$\delta(\mu\text{-}PPh_2)$	$\delta(PR_3)$	J(P–P), Hz	J(P–Rh), Hz	J(P–W), Hz
2	166.4 dd	...	33.0	107.5	161
	...	53.9 dt	33.0	163.6	...
3	190.3 d	...	...	104.0	170
4	211.0 d	...	...	135.9	180
7	202.9 d	...	...	139.2	151
	...	45.3 d	...	189.9	...
9	89.3 ddd	...	177.9, 21.7	89.0	*a*
	...	30.2 dd	178.6	139.9	...
	...	8.29 d	22.4	...	*a*
10	93.1 ddd	...	181.3, 23.2	91.6	*a*
	...	32.3 dd	181.3	139.8	...
	...	−5.6 d	23.2	...	*a*
13	206.0 d	...	...	130.0	183

[a] Unresolved.

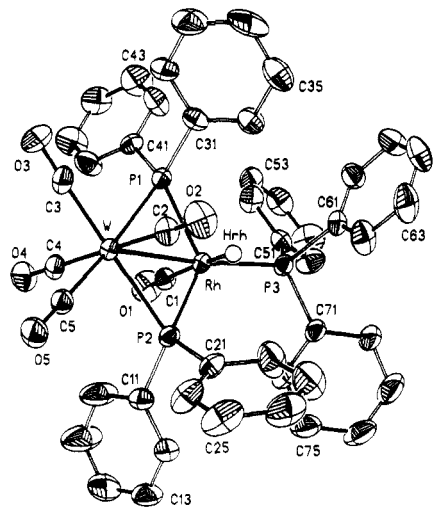

Figure 1. An ORTEP drawing and labeling scheme for **2** with 40% thermal ellipsoids.

have not been investigated, it may be that in this temperature range complex **7** undergoes a fluxional process involving a "flapping" of the bridging μ-PPh_2 ligands without Rh–P bond cleavage, similar to the behavior found for $(PEt_3)_2Rh(\mu\text{-}PPh_2)_2Rh(COD)$.[8] Complex **8** was not spectroscopically characterized but was used in the following syntheses as generated.

Protonation of the anionic complexes **7** and **8** gave the hydride complexes **2** and **3** (eq 5 and 6). Complex **2** can

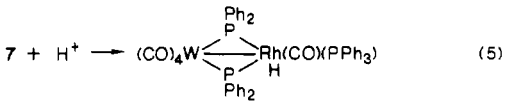

(5)

2

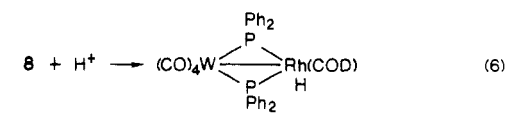

(6)

3

be isolated as a microcrystalline solid, but **3** rapidly transforms into **4** upon workup as detailed below. Both **2** and **3** were also prepared by the direct reaction of the monophosphido reagent **5** with the appropriate metal halides (eq 7 and 8). Both **2** and **3** appear to be isostructural to the corresponding W–Ir derivatives $(CO)_4\overline{W(\mu\text{-}PPh_2)_2}IrH(CO)(PPh_3)$[3] and $(CO)_4\overline{W(\mu\text{-}PPh_2)_2}IrH(COD)$[4] which have been structurally characterized. This

(5) Jardine, F. H. *Polyhedron* **1982**, *1*, 569.
(6) (a) Petersen, J. L.; Stewart, R. P., Jr. *Inorg. Chem.* **1980**, *19*, 186. (b) Carty, A. J.; Maclaughlin, S. A.; Taylor, N. J. *J. Organomet. Chem.* **1981**, *204*, C27. (c) Garrou, P. E. *Chem. Rev.* **1981**, *81*, 229. (d) Johannsen, G.; Stelzer, O. *Chem. Ber.* **1977**, *110*, 3438. (e) Carty, A. J. *Adv. Chem. Ser.* **1982**, *No. 196*, 163.
(7) (a) Mazanec, T. J.; Tau, K. D.; Meek, D. W. *Inorg. Chem.* **1980**, *19*, 85. (b) Kang, S. K.; Albright, T. A.; Wright, T. C.; Jones, R. A. *Organometallics* **1985**, *4*, 666.
(8) Kreter, P. E.; Meek, D. W. *Inorg. Chem.* **1983**, *22*, 319.

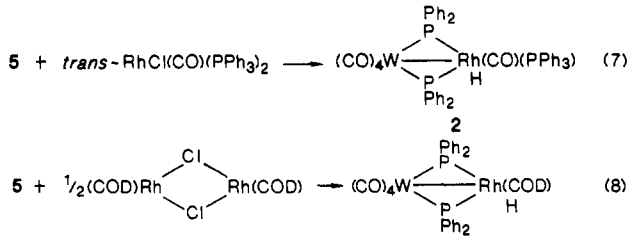

2

3

was confirmed for **2** by a complete X-ray diffraction study (Figure 1, see below). Both **2** and **3** show downfield μ-PPh_2 ^{31}P NMR resonances (Table I), implying the presence of W–Rh bonds.[6] The ^1H NMR resonance of the hydride ligand of **2** appears as a temperature-invariant (−50 → 20 °C), broad (fwhm = 3.4 Hz) triplet at δ − 12.5 with J_{P-H} = 13.5 Hz. The observed splitting of this resonance is assigned to hydride coupling to the two equivalent bridging phosphorus ligands, but the absence of resolvable hydride coupling to rhodium and the terminal phosphine is surprising. The absence of the latter was verified by recording the selectively decoupled $^{31}P\{phenyl\text{-}^1H\}$ spectrum and observing a 14.1-Hz coupling to the μ-PPh_2 ligand resonance but *no* phosphorus–hydride coupling to the terminal PPh_3 resonance. The crystal structure of **2** (Figure 1) shows the assigned structure to be correct, and we can only suggest that the Rh–H and H–P(PPh_3) couplings are ≤3 Hz and are not resolved. It should be noted that the absence of rhodium–hydride coupling was also observed in $HRh(PPh_3)_4$,[9] and Darensbourg and co-workers[10] observed unusually small P–H couplings in hydride complexes with trigonal-bipyramidal geometries similar to that of the Rh center in **2** (see below). The ^1H NMR spectrum of **3** shows the expected doublet of triplets for the hydride ligand at δ −18.1 with J_{Rh-H} and J_{P-H} = 13.3 Hz.

Although complex **3** was sufficiently stable to be spectroscopically characterized, when exposed to air or upon prolonged standing in solutions under N_2, it transformed into the cyclooctenyl complex **4** (eq 9). Complex **4** shows

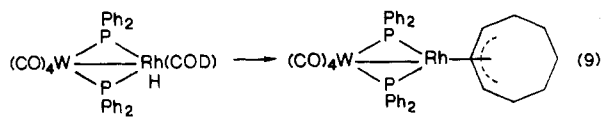

3 4

a downfield ^{31}P NMR resonance for the equivalent μ-PPh_2 ligands but does not show a hydride ^1H NMR resonance, consistent with migration of this ligand to the COD ligand. The ^1H NMR spectrum also shows resonances attributable to the cyclooctenyl ligand at δ 5.03 (br s) and 3.16 (br s) and several broad multiplets in the δ 0.5–1.5 region. For comparison, the complex $Rh(PPh_3)_2(\eta^3\text{-}C_8H_{13})$, which has a coordination environment similar to that of **4**, shows ^1H NMR resonances at δ 5.20, 3.42, and ~1.12 (br m).[10] All resonances for **4** are broad due to unresolved ^{103}Rh–^1H and ^{31}P–^1H coupling.

Phosphido Bridge Cleavage upon Reaction of 2 with Ethylene. The coordination environment of the Rh end of complex **2** superficially resembles the hydroformylation catalyst $RhH(CO)(PPh_3)_3$.[5] We were thus curious as to how the presence of an adjacent $W(CO)_4$ unit would affect the catalytic properties of the Rh center. Although complex **2** does not react with H_2, it unfortunately fragments when placed under CO and ethylene atmospheres. An unresolved mixture of products resulted from the reaction with CO, but ethylene smoothly gave the bridge-cleavage reaction shown in eq 10. Complex **9** can be isolated from

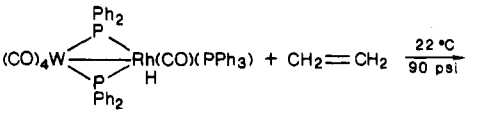

2

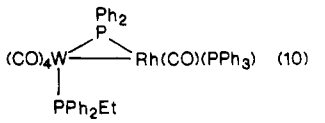

9

this reaction in modest yield as a microcrystalline yellow solid and appears similar to the corresponding W–Ir and Mo–Rh complexes prepared earlier.[3,12] Complex **9** shows separate resonances for the three different phosphorus ligands with the expected coupling pattern (Table I) and with the downfield position of the μ-PPh_2 resonance indicating the presence of a W–Rh bond.

The mechanism for this reaction presumably involves generation of an ethyl ligand on Rh by insertion of ethylene into the Rh–H bond, followed by reductive coupling of the ethyl and phosphido ligands. Evidence for this suggestion comes from two sources. First, in an attempt to prepare a methyl complex analogous to **2**, the anionic complex **7** was treated with CH_3OTf. A methyl complex did not result, but instead the PPh_2CH_3 complex **10** was formed (eq 11). Presumably the methyl group initially adds to

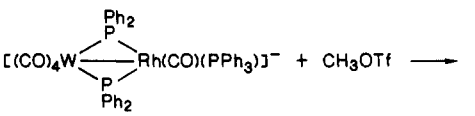

7

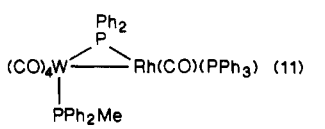

10

Rh, but with rapid subsequent methyl–phosphido coupling to give the observed product. Also, it was previously found that the relatively stable W–Ir(CH_3) complex **11** undergoes a similar reductive coupling to give complex **12** analogous to the W–Rh complex **10** (eq 12).[2a] These types of

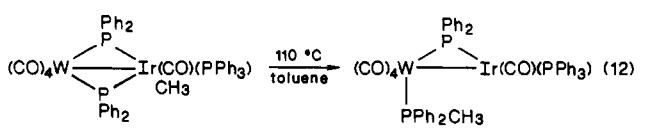

11 12

bridge-elimination reactions will surely limit the applications of phosphido-bridged complexes in catalytic reactions since many of the catalytic processes of interest involve the formation of metal–carbon bonds at intermediate stages of the reaction, and the formation of a relatively strong P–C bond provides a strong thermodynamic driving force for such bridge degradation.

Reaction of Complex 4 with CO + PPh_3 To Form Complex 2. Complex **4** was observed to rapidly react with PPh_3 under 1 atm of CO to form complex **2** in near quantitative yield (eq 13). This reaction presumably proceeds via loss of either 1,3- or 1,5-COD, but no attempt

(9) Dewhist, K. C.; Keim, W.; Reilly, C. A. *Inorg. Chem.* **1968**, *7*, 546.
(10) Ash, C. E.; Delord, T.; Simmons, D.; Darensbourg, M. Y. *Organometallics* **1986**, *5*, 17.
(11) Reilly, C. A.; Thyret, H. *J. Am. Chem. Soc.* **1967**, *89*, 5144.
(12) Roberts, D. A. Ph.D. Dissertation, The Pennsylvania State University, 1981.

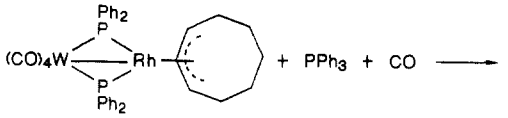

4

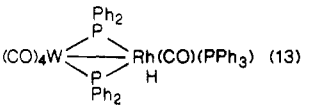

2

was made to identify the organic product.

Reaction of Complexes 3 and 4 with CO To Form the Tetranuclear Complex 13. Complex 4 reacts with CO under relatively mild conditions to give the tetranuclear complex 13, eq 14. Complex 13 has been crystallo-

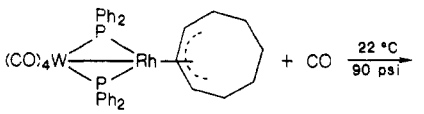

4

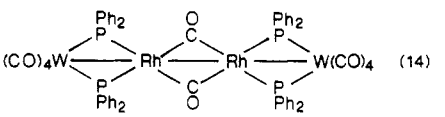

13 (47%)

graphically characterized (Figure 2), and its spectroscopic data are consistent with the determined structure. Noteworthy is the appearance of a single ^{31}P NMR resonance at δ 206 (d), implying equivalent μ-PPh_2 ligands. Complex 13 is quite stable and survives air exposure in both solution and the solid state for prolonged periods.

Insight into the mechanism by which complex 13 forms is provided by the analogous reaction of $(CO)_4W(\mu\text{-}PPh_2)_2IrH(COD)$ with CO. With Ir in place of Rh, a tetrametallic W_2Ir_2 complex is not obtained, but instead complex 15 is isolated in modest yield (eq 15).[4] A complex

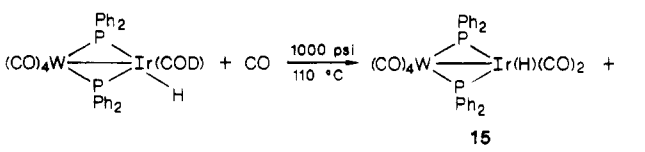

15

COD (15)

(16) similar to 15 could be an intermediate in the synthesis of 13, and the overall reaction shown in Scheme I is proposed. If we consider only the Rh end of these molecules, which is where all the chemistry described herein occurs, the stoichiometry of the proposed conversion of 16 into 14 and then into 13 is similar to established chemistry for $HRh(CO)(PPh_3)_3$ (eq 16).[5,13] Indeed, the coordination geometry of the Rh_2 portion of 13 is remarkably similar to that found in structurally characterized 17[14] (see below).

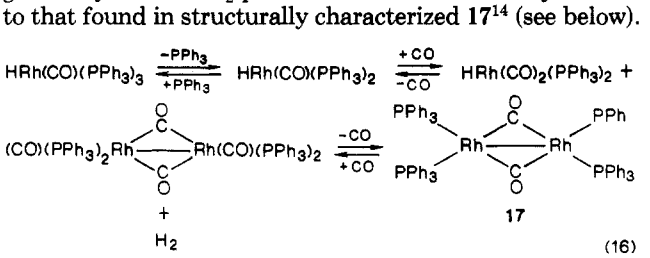

17

(16)

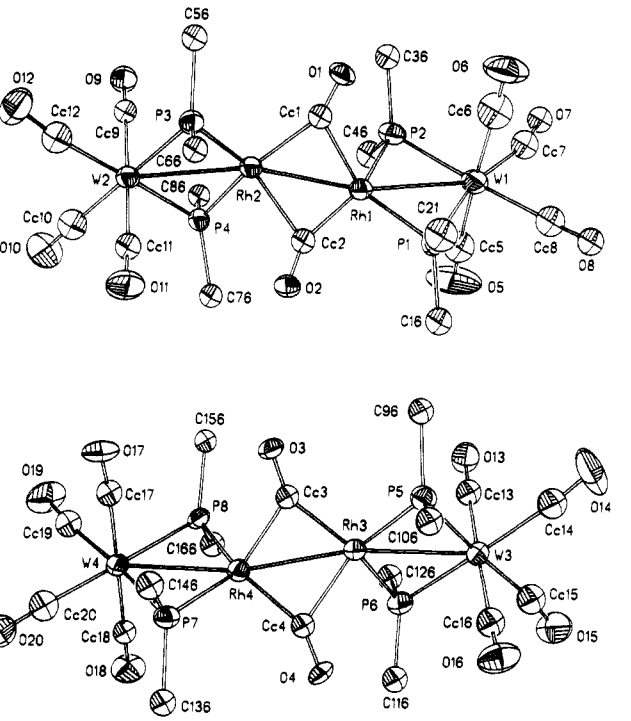

Figure 2. ORTEP diagrams and labeling schemes for the two crystallography independent molecules of 13 drawn with 40% thermal ellipsoids. The isotropic radii for the carbonyl groups 7 and 8 are arbitrary (see Experimental Section). Molecule 1 is on top, and molecule 2 is on the bottom.

Scheme I

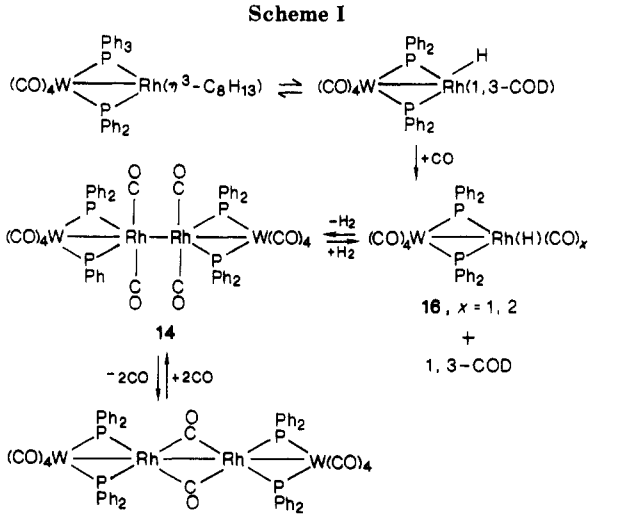

Reaction of Complex 13 with H_2/CO/PPh_3 To Yield Complex 2. Complex 13 does not react when stirred for 30 min under 100 psi of H_2 pressure in the presence of excess PPh_3, but rapid reaction ensues if CO is also present (100 psi, 4:1 H_2/CO) to give complex 2 in near quantitative yield (eq 17). It is interesting that CO is necessary for

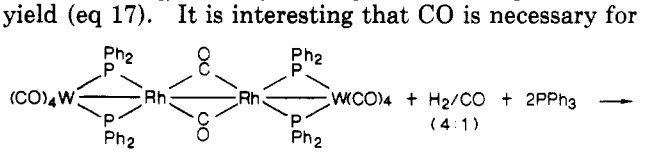

13

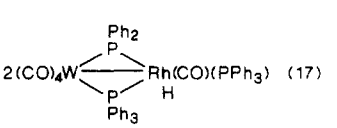

2

(17)

(13) Evans, D.; Yagupsky, G.; Wilkinson, G. *J. Chem. Soc. A* **1968**, 2660.

(14) Singh, P.; Dammann, C. B.; Hodgson, D. J. *Inorg. Chem.* **1973**, *12*, 1335.

Table II. Crystal Data Collection and Refinement Parameters for $(CO)_4\overline{W(\mu\text{-}PPh_2)_2}RhH(CO)(PPh_3)$ (2) and $[(CO)_4\overline{W(\mu\text{-}PPh_2)_2}Rh(\mu\text{-}CO)_2]_2 \cdot x CH_2Cl_2$ ($x \approx 0.5$) (13)

	2	13
formula	$C_{47}H_{36}O_5P_3RhW$	$C_{60}H_{40}O_{12}P_4Rh_2W_2$ (without solvent)
cryst system	monoclinic	triclinic
space group	$P2_1/n$	$P\bar{1}$
a, Å	11.430 (3)	11.580 (2)
b, Å	19.085 (5)	19.838 (4)
c, Å	20.738 (6)	22.299 (5)
α, deg		82.94 (2)
β, deg	100.80 (2)	79.17 (2)
γ, deg		88.63 (2)
V, Å^3	4444 (2)	5857 (2)
Z	4	4
ρ(calcd), g cm^{-3}	1.59	1.93 (with $^1/_2CH_2Cl_2$/fw)
temp, °C	22	22
cryst dimens, mm	0.26 × 0.26 × 0.31	0.12 × 0.20 × 0.24
radiation	Mo Kα (λ = 0.71073 Å)	
diffractometer	Nicolet R3	
monochromator	graphite crystal	
data correctns	*Lp*, absorption (empirical)	
μ, cm^{-1}	32.25	48.5
max/min trans	1.21	0.031/0.018
std reflctns	3 std/197 reflctns (<1% decay)	3 std/197 reflctns (<1% decay)
scan method	Wyckoff	ω
scan speed, deg/min	5–20 (var)	10
scan range, deg	$4 \le 2\theta \le 50$	$4 \le 2\theta \le 43.5$
data collected	8481	12864
unique data	8017	12334
unique data	5754 [$F_o > 4(F_o)$]	6749 [$F_o > 3\sigma(F_o)$]
F_F[2]	0.0393	0.0619
R_{wF}[a]	0.0420	0.0699
GOF	1.033	1.234
max shift/error	0.08	0.085
highest peak, final diff map, e Å^{-3}	0.59	1.24

[a] $w^{-1} = \sigma^2(F_o) + |g|(F_o)^2$; $R_F = \sum[|F_o| - |F_c|]/\sum|F_o|$; $F_{wF} = [\sum w^{1/2}(|F_o| - |F_c|)]/\sum w^{1/2}|F_o|$

this reaction to occur but is not consumed in forming **2**. Exposure of solutions of **13** to 1 atm of CO alone gave loss of the ν_{CO} bands of **13**, and new bands grew in at 2040, 2020, 1985, 1950, and 1930 cm^{-1}. Removal of the solvent and the CO atmosphere gave quantitative reformation of **13**. We suggest that **13** adds two CO molecules to form complex **14** (eq 18 and Scheme I) and that it is **14** which reacts with H_2/PPh_3 to give the observed product.

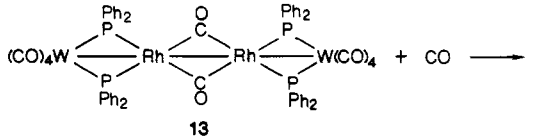

13

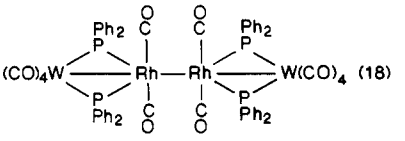

(18)

14

Structural Characterization of $(CO)_4\overline{W(\mu\text{-}PPh_2)_2}RhH(CO)(PPh_3)$ (2). An ORTEP drawing of **2** showing the atomic labeling scheme is given in Figure 1, and pertinent crystallographic details are given in Tables II and III. Selected bond lengths and angles are set out in Table IV. The W–Rh bond (2.855 (1) Å) is bridged by the two μ-PPh_2 ligands with tungsten further coordinated by four CO's and rhodium by the hydride, CO, and PPh_3 ligands. The hydride ligand was located and refined. If the W–Rh bond is ignored, the coordination geometry of W is octahedral and that of Rh is trigonal bipyramidal with the hydride ligand trans to CO. The structure is isomorphous with that of $(CO)_4\overline{W(\mu\text{-}PPh_2)}IrH(CO)(PPh_3)$ (**1**) (W–Ir = 2.8764 (6) Å).[3] The only unusual structural feature of **2** is the unrealistically short Rh–H bond length of 1.34 (7) Å (Ir–H = 1.60 (8) Å in **1**[3]). This anomaly is presumably due to the uncertainty in determining hydrogen atom positions by X-ray diffraction.

Table III. Atomic Coordinates (×10^4) and Isotropic Thermal Parameters (Å^2 × 10^3) for 2

	x	y	z	U, Å^2
W	173.3 (1)	8820.3 (1)	784.1 (1)	34.0 (1)[a]
Rh	−785.7 (5)	7515.9 (3)	1115.1 (3)	32.6 (2)[a]
P(1)	558 (2)	7597 (1)	420 (1)	36 (1)[a]
P(2)	−1157 (2)	8564 (1)	1596 (1)	39 (1)[a]
P(3)	−1074 (2)	6468 (1)	1579 (1)	39 (1)[a]
O(1)	−3058 (5)	7379 (4)	68 (3)	87 (3)[a]
O(2)	2348 (5)	8576 (3)	1964 (3)	81 (3)[a]
O(3)	2098 (5)	92463 (3)	−60 (3)	80 (3)[a]
O(4)	−1955 (5)	9142 (3)	−394 (3)	69 (2)[a]
O(5)	24 (5)	10401 (3)	1207 (3)	68 (2)[a]
C(1)	−2224 (7)	7453 (4)	454 (4)	43 (3)[a]
C(2)	1552 (6)	8661 (4)	1545 (4)	48 (3)[a]
C(3)	1380 (7)	9092 (4)	238 (4)	52 (3)[a]
C(4)	−1200 (7)	9004 (4)	34 (3)	45 (3)[a]
C(5)	69 (6)	9833 (4)	1049 (3)	45 (3)[a]
C(11)	−2677 (7)	8910 (4)	1529 (4)	51 (3)[a]
C(12)	−3193 (8)	8985 (4)	2068 (4)	66 (4)[a]
C(13)	−4385 (9)	9213 (5)	1999 (6)	81 (5)[a]
C(14)	−5032 (9)	9360 (6)	1396 (7)	94 (5)[a]
C(15)	−4520 (11)	9274 (9)	869 (6)	143 (8)[a]
C(16)	−3341 (9)	9054 (7)	930 (5)	117 (6)[a]
C(21)	−495 (7)	8728 (4)	2450 (3)	49 (3)[a]
C(22)	−184 (10)	8189 (5)	2881 (4)	97 (5)[a]
C(23)	373 (12)	8300 (7)	3528 (5)	120 (6)[a]
C(24)	618 (0)	8958 (7)	3748 (5)	94 (5)[a]
C(25)	300 (10)	9517 (6)	3331 (5)	89 (5)[a]
C(26)	−277 (8)	9398 (5)	2689 (4)	74 (4)[a]
C(31)	2095 (7)	7295 (4)	629 (4)	47 (3)[a]
C(32)	2881 (7)	7439 (5)	208 (5)	73 (4)[a]
C(33)	4047 (8)	7215 (6)	359 (6)	90 (5)[a]
C(34)	4458 (8)	6857 (7)	947 (7)	104 (6)[a]
C(35)	3688 (9)	6729 (5)	1359 (5)	86 (5)[a]
C(36)	2520 (7)	6945 (4)	1200 (4)	59 (3)[a]
C(41)	122 (7)	7287 (4)	−426 (3)	43 (3)[a]
C(42)	567 (8)	6671 (4)	−621 (4)	71 (4)[a]
C(43)	165 (10)	6406 (5)	−1249 (5)	90 (5)[a]
C(44)	−672 (9)	6723 (6)	−1669 (4)	79 (4)[a]
C(45)	−1149 (10)	7322 (6)	−1498 (4)	93 (5)[a]
C(46)	−734 (8)	7610 (5)	−871 (4)	75 (4)[a]
C(51)	−1768 (6)	5806 (4)	989 (4)	46 (3)[a]
C(52)	−1434 (8)	5773 (4)	381 (4)	61 (3)[a]
C(53)	−1884 (9)	5256 (5)	−71 (4)	69 (4)[a]
C(54)	−2667 (9)	4774 (5)	81 (5)	77 (4)[a]
C(55)	−2981 (9)	4794 (5)	667 (6)	94 (5)[a]
C(56)	−2568 (8)	5301 (4)	1128 (5)	74 (4)[a]
C(61)	280 (7)	6018 (4)	1987 (4)	46 (3)[a]
C(62)	910 (9)	6268 (5)	2576 (4)	73 (4)[a]
C(63)	1967 (10)	5947 (6)	2886 (5)	87 (4)[a]
C(64)	2401 (9)	5391 (5)	2590 (5)	80 (4)[a]
C(65)	1785 (8)	5140 (5)	2015 (5)	76 (4)[a]
C(66)	743 (7)	5447 (4)	1721 (4)	60 (3)[a]
C(71)	−1977 (7)	6486 (4)	2210 (4)	50 (3)[a]
C(72)	−1872 (9)	5994 (4)	2714 (4)	71 (4)[a]
C(73)	−2586 (12)	6043 (6)	3181 (5)	103 (6)[a]
C(74)	−3387 (11)	6561 (5)	3178 (5)	94 (5)[a]
C(75)	−3529 (9)	7037 (5)	2668 (5)	85 (5)[a]
C(76)	−2818 (7)	7005 (4)	2191 (4)	62 (3)[a]
HRh	149 (75)	7520 (40)	1611 (39)	72 (28)

[a] Equivalent isotropic U defined as one-third of the trace of the orthogonalised U_{ij} tensor.

Structural Characterization of 13. Complex **13** crystallizes in the triclinic space group $P\bar{1}$ with two independent but similar molecules per unit cell. These are

Table IV. Selected Bond Distances and Angles for $(CO)_4W(\mu\text{-}PPh_2)_2Rh(PPh_3)(CO)(H)$

(a) Bond Distances

W–Rh	2.855 (1)	W–C(5)	2.018 (7)
W–P(1)	2.518 (2)	Rh–P(1)	2.300 (2)
W–P(2)	2.519 (2)	Rh–P(2)	2.309 (2)
W–C(2)	2.033 (7)	Rh–P(3)	2.270 (2)
W–C(3)	2.009 (9)	Rh–C(1)	1.936 (7)
W–C(4)	2.022 (7)	Rh–H(Rh)	1.34 (7)

(b) Bond Angles

P(1)–W–P(2)	100.4 (1)	C(2)–W–C(5)	90.5 (3)
P(1)–Rh–P(2)	114.3 (1)	C(3)–W–C(4)	92.2 (3)
W–P(1)–Rh	72.5 (1)	C(3)–W–C(5)	89.3 (3)
Wp–P(2)–Rh	72.4 (1)	C(4)–W–C(5)	88.1 (3)
P(1)–W–C(2)	86.6 (2)	P(1)–Rh–P(3)	119.4 (1)
P(1)–W–C(3)	83.9 (2)	P(1)–Rh–C(1)	98.0 (2)
P(1)–W–C(4)	94.8 (2)	P(1)–Rh–H(Rh)	87 (4)
P(1)–W–C(5)	172.7 (2)	P(2)–Rh–P(3)	121.8 (1)
P(2)–W–C(2)	86.0 (2)	P(2)–Rh–C(1)	99.1 (2)
P(2)–W–C(3)	172.1 (2)	P(2)–Rh–H(Rh)	81 (3)
P(3)–W–C(4)	94.0 (2)	P(3)–Rh–C(1)	94.2 (2)
P(3)–W–C(5)	86.0 (2)	P(3)–Rh–H(Rh)	81 (3)
C(2)–W–C(3)	87.8 (3)	C(1)–Rh–H(Rh)	174 (4)
C(2)–W–C(4)	178.6 (3)		

shown in the ORTEP drawings in Figure 2 which also gives the labeling schemes used. Pertinent crystallographic details are given in Tables II and V. Selected bond lengths and angles are set out in Table VI. The four metal atoms are arranged in a bent chain with the two Rh atoms in the middle of the chain. Although not crystallographically imposed, the two molecules are enantiomers with the asymmetry created by the bending of the metal chain. This can be seen by close inspection of Figure 2 but is illustrated in a more exaggerated fashion in the drawings below.

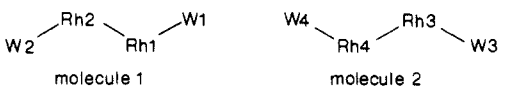

Table VII lists several of the important dihedral angles for the two molecules as well as the torsional angles for the tetrametal chain. Note that the torsional angles for the two molecules are in the opposite sense. The $W(\mu\text{-}P)_2Rh$ portions of the molecule are essentially planar, although the central $Rh(\mu\text{-}C)_2Rh$ unit is bent with [Rh–Cc–Rh]–[Rh–Cc–Rh] dihedral angles of 129.7 (3)° and 135.7 (3)°, respectively, for molecules 1 and 2.

The metal–metal distances for the two molecules are all within normal bonding values. For example, the Rh–Rh distances of 2.635 (3) and 2.658 (3) Å compare well to the 2.630 (1) Å distance in **17**[14] and to the 2.6649 (4) Å distance in $[Cp(CO)Rh]_2(\mu\text{-}CH_2)$.[15] Although a Rh=Rh double bond could be invoked to achieve 18-electron configurations at each Rh, the Rh—Rh distance is longer than the established Rh=Rh double bond distances of 2.550 (1) Å in $[Rh(\mu\text{-}P\text{-}t\text{-}Bu_2)(CO)(PMe_3)]_2$[16a] and 2.552 (2) Å in $[Rh(\mu\text{-}PH\text{-}t\text{-}Bu)(PMe_3)_2]_2$.[16b] The four W–Rh distances average 2.812 Å and compare well to those found in $RhW(\mu\text{-}CR)(CO)_2(PMe_3)Cp(\eta\text{-}C_9H_7)$ (2.796 (1) Å[17a]), $RhW(\mu\text{-}C(Tol)C(Ph)C(Ph))(CO)_2Cp(\eta\text{-}C_9H_7)$ (2.754 (1) Å[17b]), and $Rh_2W(\mu\text{-}CTol)(acac)_2(CO)_3Cp$ (2.809 (2) Å[17c]).

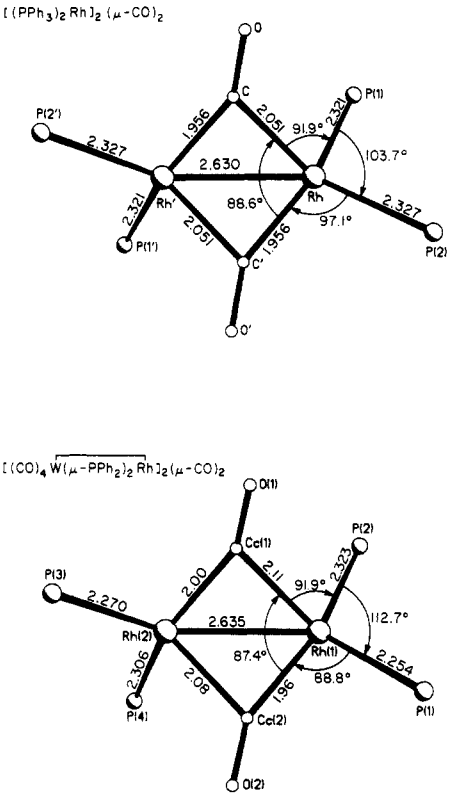

Figure 3. A comparison of the Rh_2 core of molecule 1 of complex **13** and $[Rh(PPh_3)_2]_2(\mu\text{-}CO)_2$ (**17**).[12]

The geometry about the binuclear Rh_2 unit in **13** is remarkably similar to that found in the related binuclear complex $[Rh(PPh_3)_2]_2(\mu\text{-}CO)_2$ (**17**).[14] This is well-illustrated by the ORTEP drawings in Figure 3 which compare the Rh_2 cores of molecule 1 of **13** and complex **17**, drawn from similar perspectives. The only significant deviation is in the P–Rh–P bond angles which average 112.4° in **13** and is 103.7 (1)° in **17**. The ~8° opening of this angle in tetranuclear **13** is presumably a consequence of the presence of the adjacent W centers.

Although assignment of formal oxidation states to phosphido-bridged complexes such as these is dissicult, the molecule appears best described as having W(0) and Rh(II) centers with a single metal–metal bond between the Rh atoms and with donor–acceptor W–Rh bonds. If we adopt the electron-counting convention that assigns zero oxidation states to all atoms, the $\mu\text{-}PPh_2$ ligands are net three-electron donors and the W center achieves 18e by combination of its six electrons with eight from the carbonyls and two from each of the phosphido bridges. The W center then serves as a two-electron donor to its adjacent Rh. The Rh center achieves 16e by combining its nine electrons with the two donated from W, two from the two phosphido bridges, two from the two bridging carbonyls, and one from the Rh–Rh bond.

Experimental Section

The complexes $W(CO)_4(PPh_2H)_2$,[3,18] *trans*-$RhCl(CO)(PPh_3)_2$,[19] and $[Rh(\mu\text{-}Cl)(COD)]_2$ (COD = 1,5-cyclooctadiene)[20] were prepared according to literature procedures. Methyl triflate (CH_3OTf) and *n*-butyllithium were purchased from Aldrich Chem. Co. and used

(15) Herrmann, W. A.; Kruger, C.; Goddard, R.; Bernal, I. *J. Organomet. Chem.* **1977**, *140*, 73.
(16) (a) Jones, R. A.; Wright, T. C. *Organometallics* **1983**, *2*, 1842. (b) Jones, R. A.; Norman, N. C.; Seeberger, M. H.; Atwood, J. L.; Hunter, W. E. *Organometallics* **1983**, *2*, 1629.
(17) (a) Jeffery, J. C.; Sambale, C.; Schmidt, M. F.; Stone, F. G. A. *Organometallics* **1982**, *1*, 1597. (b) Chetcuti, M. J.; Chetcuti, P. A. M.; Jeffery, J. C.; Mills, R. M.; Mitrprachachon, P.; Pickering, S. J.; Stone, F. G. A.; Woodward, P. *J. Chem. Soc., Dalton Trans.* **1982**, 699. (c) Green, M.; Howard, J. A. K.; Porter, S. J.; Stone, F. G. A.; Tyler, D. C. *J. Chem. Soc., Dalton Trans.* **1984**, 2553.
(18) Keiter, R. L.; Sun, Y. Y.; Brodack, J. W.; Cary, L. W. *J. Am. Chem. Soc.* **1979**, *101*, 2638.
(19) Evans, D.; Osborn, J. A.; Wilkinson, G. *Inorg. Synth.* **1968**, *11*, 99.
(20) Giordano, G.; Crabtree, R. H. *Inorg. Synth.* **1979**, *19*, 218.

as received. Hydrocarbon and ether solvents were predried with CaH_2 and distilled from sodium–benzophenone ketyl under N_2 prior to use. All reactions were carried out under an atmosphere of prepurified N_2 using standard Schlenk techniques. Instruments used in this work have been previously described.[3,4]

Preparation of $(CO)_4\overline{W(\mu\text{-}PPh_2)_2}Rh(H)(CO)(PPh_3)$ (2). Method A. A yellow THF (30-mL) solution of *trans*-$RhCl(CO)(PPh_3)_2$ (450 mg, 0.651 mmol) was added dropwise to a stirred THF (40-mL) solution of $Li[W(CO)_4(PPh_2H)(PPh_2)]$, generated in situ by addition of 1.1 equiv of *n*-BuLi to $W(CO)_4(PPh_2H)_2$ (396 mg, 0.593 mmol). The red solution was stirred for 1.5 h, after which time the THF was evaporated to yield a reddish oil. The oil was extracted with toluene until the extracts were colorless. The combined extracts were filtered through Celite and concentrated to approximately 5 mL. Diethyl ether (20 mL) and petroleum ether (25 mL) were added, and the flask was cooled to −60 °C. The red crystals which formed over a period of several days were isolated by filtration to give a 27% yield of **2** (172 mg, 0.162 mmol). **2**: IR (CH_2Cl_2) ν_{CO} 2030 (s), 1935 (vs), 1915 (vs) cm^{-1}; ^1H NMR (C_6D_6) δ −12.5 (t, Rh–H, $J_{H\text{-}P}$ = 13.5 Hz); MS (EI), m/z 1060 (M^+), 1032 (M^+ − CO), 976 (M^+ − 3CO), 948 (M^+ − 4CO), 920 (M^+ − 5CO). Anal. Calcd for $C_{47}H_{36}O_5P_3RhW$: C, 53.22; H, 3.43. Found: C, 53.48; H, 3.34.

Method B. $Li_2[W(CO)_4(PPh_2)_2]$, generated in situ by the addition of *n*-BuLi (1.074 mL of a 1.6 M solution in hexanes, 1.72 mmol) to a 0 °C Et_2O (50 mL) solution of $W(CO)_4(PPh_2H)_2$ (547 mg, 0.818 mmol), was added dropwise to a stirred Et_2O (50 mL) slurry of *trans*-$RhCl(CO)(PPh_3)_2$ (565 mg, 0.818 mmol) at room temperature. The resultant red solution of $Li[(CO)_4\overline{W(\mu\text{-}PPh_2)_2}Rh(CO)(PPh_3)]$ (**7**) [IR (THF) ν_{CO} 2003 (s), 1899 (vs), 1870 (vs) cm^{-1}] was stirred overnight, after which time *p*-toluenesulfonic acid (155 mg, 0.900 mmol) was added. The resultant cherry-red solution was filtered through Celite and the Celite washed with Et_2O until the ether washings were colorless. The combined extracts were concentrated to approximately 25 mL and cooled to −78 °C to induce crystallization of red **2**. The microcrystals were collected by filtration, washed once with hexanes (10 mL), and dried to give **2** in 51% yield (441 mg, 0.416 mmol).

Preparation of $(CO)_4\overline{W(\mu\text{-}PPh_2)_2}Rh(H)(COD)$ (3). The salt $Li[W(CO)_4(PPh_2H)(PPh_2)]$(0.203 mmol), generated in situ in THF (30 mL), was added to a yellow THF solution (20 mL) of $[Rh(\mu\text{-}Cl)(COD)]_2$ while being stirred at room temperature. After 15 min the IR spectrum showed only bands attributed to $(CO)_4\overline{W(\mu\text{-}PPh_2)_2}Rh(H)(COD)$: ν_{CO} 2035 (s), 1946 (vs), 1908 (vs) cm^{-1}. Air exposure of the IR sample caused complete conversion to **4**. The THF was removed in vacuo, at or below room temperature, and Et_2O (30 mL) was distilled into the flask. The resultant orange solution was filtered through Celite and then evaporated to dryness. The residue was dissolved in 1 g of C_6D_6 for NMR measurements. **3**: ^1H NMR (C_6D_6) δ 4.83 (br s, 2 H), 3.43 (br s, 2 H), 1–2 (m, br, 8 H), −18.1 (dt, $J_{P_\mu\text{-}H} \approx J_{Rh\text{-}H}$ = 13.3 Hz).

Preparation of $(CO)_4\overline{W(\mu\text{-}PPh_2)_2}Rh(C_8H_{13})$ (4). Method A. The salt $Li[W(CO)_4(PPh_2H)(PPh_2)]$ (1.01 mmol), generated in situ by addition of 1.0 equiv of *n*-BuLi to a THF (25-mL) solution of $W(CO)_4(PPh_2H)_2$ (678 mg, 1.01 mmol), was added dropwise to a yellow THF solution of $[Rh(\mu\text{-}Cl)(COD)]_2$ (250 mg, 0.507 mmol) while being stirred. The solution turned red and showed principal IR bands at 2033 (vs), 1945 (vs), and 1908 (vs) cm^{-1}. The THF was removed under vacuum, and the resultant red residue was extracted with ether until the ether extracts were colorless. The combined extracts were filtered through Celite and then evaporated to dryness in air, yielding 657 mg (0.748 mmol, 73.8%) of **4** as a dark red microcrystalline powder. **4**: IR (CH_2Cl_2) ν_{CO} 2035 (s), 1948 (vs), 1925 (s) cm^{-1}; ^1H NMR (C_6D_6) δ 5.03 (br s, 1 H), 3.16 (br s, 2 H), 2.0–0.5 (br m); MS (EI) m/z 878 (M^+), 850 (M^+ − CO), 822 (M^+ − 2CO), 794 (M^+ − 3CO), 766 (M^+ − 4CO), 742 (M^+ − CO − COD), 714 (M^+ − 2CO − COD), 686 (M^+ − 3CO − COD), 658 (M^+ − 4CO − COD). Anal. Calcd for $C_{36}H_{33}O_4P_2RhW$: C, 49.23; H, 3.75. Found: C, 49.02; H, 4.10.

Method B. $Li_2[W(CO)_4(PPh_2)_2]$ (0.949 mmol) in Et_2O, generated in situ by the addition of 2.0 equiv of *n*-BuLi to $W(CO)_4(PPh_2H)_2$ (634 mg, 0.949 mmol), was added dropwise to a yellow slurry of $[Rh(\mu\text{-}Cl)(COD)]_2$ (230 mg, 0.475 mmol) in Et_2O (10 mL). The resultant dark red solution of $Li[(CO)_4W(\mu\text{-}PPh_2)_2Rh(COD)]$ (**8**) was stirred for 2 h after which time *p*-toluenesulfonic acid in THF was added dropwise until all the IR bands for **8** (1995 (m), 1893 (vs, br), 1873 (sh) cm^{-1}) disappeared. The reaction mixture was filtered through Celite to remove the salts, and the Et_2O was removed in vacuo to yield 664 mg of **4** (0.756 mmol, 80%) as a dark red powder. This material was further purified, with some decomposition, by extraction with isopentane in a Soxhlet extractor, followed by recrystallization from Et_2O.

Reaction of 2 with Ethylene. Complex **2** (0.104 g, 0.0981 mmol) was dissolved in CH_2Cl_2 (3 mL) in a 90-mL Fisher-Porter glass reaction vessel. The vessel was purged twice with ethylene (Matheson CP grade) and then pressurized to 90 psig while being stirred. Over the course of 1 h the initially red solution turned yellow. The solvent was removed in vacuo and the residue chromatographed on basic Al_2O_3 with hexane/CH_2Cl_2 (75/25) as eluant. A single yellow band eluted from which $(PPh_2C_2H_5)(CO)_4\overline{W(\mu\text{-}PPh_2)}Rh(CO)(PPh_3)$ (**9**) was isolated as yellow microcrystals upon evaporation of solvent (28.3 mg, 26.5%). **9**: IR (CH_2Cl_2) ν_{CO} 2018 (w), 1900 (s), 1912 (vs), 1825 (w) cm^{-1}. Anal. Calcd for $C_{49}H_{40}O_5P_3RhW$: C, 54.04; H, 3.71. Found: C, 53.98; H, 4.14.

Reaction of 7 with $CH_3OSO_2CF_3$. A yellow solution (Et_2O, 25 mL) of $Li_2[W(CO)_4(PPh_2)_2]$ (0.145 mmol) was added to a slurry of *trans*-$RhCl(CO)(PPh_3)_2$ (0.100 g, 0.145 mmol) in Et_2O and stirred for 4 h. The Et_2O was then removed by evaporation, and THF (25 mL) was distilled into the flask. The resultant red solution of **7** was cooled to −78 °C, and methyl triflate (32.8 μL, 0.290 mmol) was added, causing the solution to turn brown. The solution was stirred for 1 h and the THF removed by evaporation. The remaining residue was extracted with Et_2O (3 × 20 mL), and the combined extracts were filtered through Celite and concentrated to yield a dark brown solid residue. One yellow band of **10** eluted upon chromatography on basic Al_2O_3 with hexane/CH_2Cl_2 (80/20) as eluant. Complex **10** was spectroscopically characterized: IR (CH_2Cl_2) ν_{CO} 2012 (w), 1955 (s), 1912 (vs), 1820 (w) cm^{-1}; ^1H NMR (C_6D_6) δ 1.96 (d, W–PPh_2CH_3, $J_{H\text{-}P}$ = 7.32 Hz).

Reaction of 4 with CO/PPh_3. Carbon monoxide (1 atm) was added to a stirred degassed solution (THF, 10 mL) of **4** (27 mg, 0.0307 mmol) and PPh_3 (250 mg, 0.954 mmol). After 2 h, IR and ^1H and ^{31}P NMR spectra showed only **2** to be present.

Preparation of $[(CO)_4\overline{W(\mu\text{-}PPh_2)}Rh(\mu\text{-}CO)]_2$ (13). Complex **4** (109 mg, 0.124 mmol) was dissolved in 20 mL of CH_2Cl_2 at room temperature in a 90-mL Fischer-Porter glass reaction vessel. The vessel was purged twice with CO (Matheson CP grade), pressurized to 90 psig, and stirred for 4 h. The gas was vented, the solvent was removed by evaporation, and the dark brown residue was chromatographed on basic alumina. Elution with CH_2Cl_2/hexane (20/80) gave a green band containing a presently unidentified compound, followed by a dark brown band from which brown microcrystals of **13** were isolated by solvent evaporation (46.9 mg, 0.0294 mmol, 47.3%). **13**: IR (CH_2Cl_2) ν_{CO} 2043 (s), 1964 (s), 1946 (vs), 1848 (vw), 1825 (w) cm^{-1}; MS (FD), m/z 1594 (M^+). Anal. Calcd for $C_{58}H_{40}O_{10}P_4Rh_2W_2$: C, 43.69; H, 2.53. Found: C, 44.44; H, 2.76.

Reaction of 13 with H_2/CO/PPh_3. Complex **13** (10.9 mg, 0.00684 mmol) and 18 mg (0.0684 mmol) of PPh_3 were dissolved in CH_2Cl_2 (10 mL) in a 90-mL Fisher-Porter glass reaction vessel to give a yellow solution. The vessel was purged four times with H_2 (100 psi) and then pressurized to 100 psi of H_2. After 30 min the IR spectrum showed no change. The H_2 was vented to 80 psi and the vessel repressurized to 100 psi with CO. After 30 min the solution was pink and the IR spectrum showed quantitative conversion to **2**.

X-ray Diffraction Study of $[(CO)_4\overline{W(\mu\text{-}PPh_2)_2}Rh(\mu\text{-}CO)]_2$ (13). Dark red crystals of complex **13** were grown by slow evaporation of a heptane/CH_2Cl_2 solution and affixed to a glass fiber. Preliminary photographic data showed the data collection specimen to be of satisfactory diffraction quality. (Very low quality crystals of a monoclinic version were obtained from toluene: $P2_1/c$, a = 23.96 Å, b = 19.89 Å, c = 13.26 Å, β = 94.74°, V = 6300 Å^3, Z = 4.) Pertinent crystal and intensity data are

Table V. Atomic Coordinates (×10⁴) and Temperature Factors (Å² × 10³) for 13

atom	x	y	z	U_{eq}	atom	x	y	z	U_{eq}
W(1)	1049 (1)	430 (1)	1146 (1)	91 (1)[a]	C(44)	1587 (14)	−2284 (8)	2408 (8)	119 (12)
W(2)	3878 (1)	857 (1)	4004 (1)	52 (1)[a]	C(45)	1114 (14)	−1652 (8)	2399 (8)	86 (9)
W(3)	8906 (1)	4380 (1)	3952 (1)	53 (1)[a]	C(46)	1672 (14)	−1062 (8)	2180 (8)	76 (8)
W(4)	6057 (1)	5607 (1)	1061 (1)	51 (1)[a]	C(51)	679 (12)	903 (7)	4408 (7)	60 (7)
Rh(1)	2132 (1)	683 (1)	2050 (1)	50 (1)[a]	C(52)	−271 (12)	851 (7)	4780 (7)	84 (9)
Rh(2)	2711 (2)	827 (1)	3091 (1)	47 (1)[a]	C(53)	−684 (12)	1407 (7)	5070 (7)	73 (8)
Rh(3)	7803 (1)	4672 (1)	2995 (1)	46 (1)[a]	C(54)	−148 (12)	2009 (7)	4988 (7)	78 (8)
Rh(4)	7136 (1)	5041 (1)	1955 (1)	47 (1)[a]	C(55)	802 (12)	2062 (7)	4617 (7)	73 (8)
P(1)	2218 (6)	1339 (4)	1142 (3)	62 (3)[a]	C(56)	1215 (12)	1509 (7)	4327 (7)	53 (7)
P(2)	1067 (5)	−239 (4)	2154 (4)	66 (3)[a]	C(61)	2958 (14)	2877 (10)	3940 (6)	86 (9)
P(3)	2432 (5)	1558 (3)	3813 (3)	50 (3)[a]	C(62)	3204 (14)	3551 (10)	3715 (6)	93 (10)
P(4)	4083 (5)	137 (3)	3173 (3)	52 (3)[a]	C(63)	3137 (14)	3797 (10)	3110 (6)	93 (10)
P(5)	7521 (5)	3763 (3)	3735 (3)	55 (3)[a]	C(64)	2825 (14)	3368 (10)	2731 (6)	103 (11)
P(6)	9133 (5)	5325 (3)	3115 (3)	56 (3)[a]	C(65)	2580 (14)	2694 (10)	2956 (6)	70 (8)
P(7)	7120 (5)	4592 (3)	1062 (3)	53 (3)[a]	C(66)	2646 (14)	2449 (10)	3561 (6)	47 (6)
P(8)	6090 (5)	5978 (3)	2070 (3)	51 (3)[a]	C(71)	5904 (14)	647 (7)	2455 (7)	72 (8)
O(1)	555 (12)	1165 (9)	2982 (8)	72 (8)[a]	C(72)	6671 (14)	700 (7)	1939 (7)	93 (10)
O(2)	4046 (12)	1464 (8)	2008 (8)	69 (8)[a]	C(73)	6710 (14)	250 (7)	1501 (7)	79 (8)
O(3)	5619 (11)	4391 (8)	2947 (8)	63 (7)[a]	C(74)	5982 (14)	−253 (7)	1579 (7)	81 (9)
O(4)	9190 (12)	4414 (9)	1867 (8)	72 (8)[a]	C(75)	5215 (14)	−307 (7)	2095 (7)	68 (7)
O(5)	2865 (18)	−407 (14)	511 (14)	184 (16)[a]	C(76)	5176 (14)	143 (7)	2533 (7)	53 (7)
O(6)	−878 (15)	1224 (12)	1725 (12)	163 (14)[a]	C(81)	4679 (10)	−1190 (9)	3489 (8)	84 (9)
O(7)	−505 (30)	−594 (26)	945 (25)	457 (39)[a]	C(82)	4502 (10)	−1878 (9)	3692 (8)	100 (9)
O(8)	898 (34)	1428 (31)	−105 (16)	374 (40)[a]	C(83)	3533 (10)	−2137 (9)	3780 (8)	117 (11)
O(9)	2625 (14)	−363 (10)	4823 (8)	83 (9)[a]	C(84)	2741 (10)	−1710 (9)	3667 (8)	92 (9)
O(10)	5887 (16)	165 (13)	4244 (11)	139 (13)[a]	C(85)	2918 (10)	−1022 (9)	3464 (8)	81 (8)
O(11)	5120 (15)	2129 (9)	3254 (10)	93 (9)[a]	C(86)	3887 (10)	−762 (9)	3376 (8)	52 (6)
O(12)	3612 (16)	1515 (10)	5236 (8)	107 (10)[a]	C(91)	5894 (12)	3048 (6)	4535 (8)	75 (8)
O(13)	7542 (14)	5381 (9)	4766 (8)	88 (9)[a]	C(92)	4945 (12)	3007 (6)	4907 (8)	96 (10)
O(14)	8538 (21)	3436 (11)	5225 (10)	149 (13)[a]	C(93)	4389 (12)	3597 (6)	5006 (8)	69 (8)
O(15)	10901 (15)	4953 (12)	4231 (9)	128 (12)[a]	C(94)	4782 (12)	4228 (6)	4732 (8)	82 (9)
O(16)	10226 (14)	3298 (9)	3209 (9)	106 (10)[a]	C(95)	5731 (12)	4269 (6)	4359 (8)	71 (8)
O(17)	4301 (12)	4577 (8)	1622 (8)	74 (8)[a]	C(96)	6287 (12)	3679 (6)	4260 (8)	53 (6)
O(18)	7816 (14)	6624 (9)	446 (9)	93 (9)[a]	C(10)	7528 (13)	2842 (8)	2884 (7)	63 (7)
O(19)	4425 (16)	6766 (11)	986 (11)	134 (12)[a]	C(102)	7679 (13)	2208 (8)	2672 (7)	106 (11)
O(20)	6010 (15)	5275 (13)	−265 (10)	127 (12)[a]	C(103)	8036 (13)	1667 (8)	3034 (7)	81 (9)
Cc(1)	1359 (19)	1012 (12)	2877 (11)	50 (7)	C(104)	8242 (13)	1761 (8)	3608 (7)	87 (9)
Cc(2)	3314 (17)	1157 (10)	2178 (10)	51 (6)	C(105)	8090 (13)	2395 (8)	3820 (7)	85 (9)
Cc(3)	6446 (17)	4552 (11)	2781 (11)	46 (7)	C(106)	7733 (13)	2935 (8)	3458 (7)	54 (7)
Cc(4)	8410 (18)	4612 (11)	2060 (11)	48 (7)	C(111)	11038 (15)	4997 (7)	2489 (8)	75 (9)
Cc(5)	2240 (24)	−101 (15)	754 (15)	100 (10)	C(112)	1182 (15)	5115 (7)	2026 (8)	77 (9)
Cc(6)	−203 (27)	927 (17)	1510 (17)	116 (12)	C(113)	11965 (15)	5716 (7)	1624 (8)	84 (9)
Cc(7)	39 (39)	−142 (25)	937 (24)	211 (21)	C(114)	11202 (15)	6201 (7)	1685 (8)	83 (10)
Cc(8)	958 (53)	1013 (35)	301 (33)	291 (34)	C(115)	10357 (15)	6083 (7)	2148 (8)	77 (9)
Cc(9)	3042 (18)	93 (11)	4533 (11)	50 (7)	C(116)	10275 (15)	5482 (7)	2550 (8)	64 (8)
Cc(10)	5167 (22)	416 (14)	4167 (13)	83 (9)	C(121)	7858 (13)	6436 (9)	3364 (8)	76 (8)
Cc(11)	4691 (18)	1643 (12)	3501 (11)	55 (7)	C(122)	7619 (13)	7070 (9)	3561 (8)	100 (10)
Cc(12)	3779 (21)	1297 (13)	4766 (14)	78 (8)	C(123)	8345 (13)	7443 (9)	3744 (8)	94 (10)
Cc(13)	8051 (19)	5022 (12)	4452 (12)	62 (8)	C(124)	9311 (13)	7182 (9)	3730 (8)	120 (12)
Cc(14)	8711 (21)	3756 (14)	4771 (14)	76 (8)	C(125)	9550 (13)	6547 (9)	3532 (8)	94 (10)
Cc(15)	10168 (22)	4724 (14)	4172 (14)	81 (9)	C(126)	8824 (13)	6174 (9)	3349 (8)	67 (7)
Cc(16)	9797 (20)	3688 (12)	3450 (12)	66 (8)	C(131)	8484 (12)	4894 (7)	−69 (8)	65 (7)
Cc(17)	4939 (18)	4943 (11)	1445 (11)	54 (7)	C(132)	9304 (12)	4743 (7)	−510 (8)	80 (9)
Cc(18)	7173 (17)	6275 (10)	673 (10)	52 (6)	C(133)	9887 (12)	4169 (7)	−396 (8)	84 (9)
Cc(19)	5035 (18)	6338 (12)	972 (11)	66 (7)	C(134)	9650 (12)	3748 (7)	159 (8)	92 (9)
Cc(20)	6010 (19)	5415 (12)	217 (12)	74 (8)	C(135)	8830 (12)	3899 (7)	600 (8)	82 (8)
C(11)	3361 (14)	1751 (9)	−9 (10)	102 (10)	C(136)	8246 (12)	4472 (7)	487 (8)	53 (6)
C(12)	4213 (14)	1755 (9)	−470 (10)	118 (12)	C(141)	6021 (13)	3432 (8)	1665 (6)	66 (7)
C(13)	5046 (14)	1365 (9)	−366 (10)	144 (11)	C(142)	5525 (13)	2821 (8)	1681 (6)	86 (9)
C(14)	5028 (14)	971 (9)	199 (10)	120 (12	C(143)	5483 (13)	2557 (8)	1135 (6)	83 (9)
C(15)	4177 (14)	967 (9)	659 (10)	77 (9)	C(144)	5937 (13)	2904 (8)	572 (6)	99 (10)
C(16)	3343 (14)	1357 (9)	555 (10)	64 (7)	C(145)	6433 (13)	3516 (8)	557 (6)	82 (8)
C(21)	1942 (19)	2246 (8)	1212 (10)	85 (9)	C(146)	6475 (13)	3780 (8)	1103 (6)	55 (7)
C(22)	2612 (19)	2787 (8)	1030 (10)	104 (10)	C(151)	5091 (10)	6008 (8)	3284 (8)	74 (8)
C(23)	2307 (19)	3442 (8)	1149 (10)	105 (10)	C(152)	4258 (0)	5957 (8)	3760 (8)	80 (8)
C(24)	1332 (19)	3555 (8)	1451 (10)	131 (13)	C(153)	3303 (10)	5877 (8)	3632 (8)	74 (8)
C(25)	662 (19)	3014 (8)	1634 (10)	163 (17)	C(154)	3182 (10)	5848 (8)	3029 (8)	80 (8)
C(26)	967 (19)	2360 (8)	1515 (10)	154 (15)	C(155)	4015 (10)	5899 (8)	2553 (8)	74 (8)
C(31)	−1035 (16)	−298 (9)	2590 (7)	74 (9)	C(156)	4970 (10)	5979 (8)	2680 (8)	48 (6)
C(32)	−1894 (16)	−389 (9)	3045 (7)	86 (10)	C(161)	6097 (10)	7347 (10)	2259 (8)	74 (8)
C(33)	−1807 (16)	−548 (9)	3660 (7)	82 (10)	C(162)	6544 (10)	7980 (10)	2217 (8)	92 (10)
C(34)	−861 (16)	−617 (9)	3819 (7)	70 (8)	C(163)	7570 (10)	8059 (10)	1993 (8)	105 (10)
C(35)	−2 (16)	−526 (9)	3364 (7)	68 (9)	C(164)	8149 (10)	7503 (10)	1811 (8)	93 (9)
C(36)	−89 (16)	−366 (9)	2749 (7)	62 (8)	C(165)	7701 (10)	6869 (10)	1853 (8)	71 (8)
C(41)	2703 (14)	−1105 (8)	1969 (8)	79 (8)	C(166)	6675 (10)	6791 (10)	2077 (8)	64 (7)
C(42)	3176 (14)	−1737 (8)	1978 (8)	96 (10)	C1(1)	8081 (20)	2080 (12)	9376 (12)	315 (14)
C(43)	2618 (14)	−2326 (8)	2197 (8)	111 (12)	C1(2)	8300 (21)	1692 (14)	10443 (14)	355 (16)
					C(170)	9062 (78)	2214 (49)	9698 (45)	408 (53)

[a] Equivalent isotropic U defined as one-third of the trace of the orthogonalized U_{ij} tensor.

Table VI. Selected Bond Distances and Angles for $[(CO)_4\overline{W(\mu\text{-}PPh_2)}Rh(\mu\text{-}CO)_2]_2$ (13)

molecule 1		molecule 2	
	(a) Distances (Å)		
W(1)–Rh(1)	2.808 (3)	W(3)–Rh(3)	2.826 (2)
W(2)–Rh(2)	2.812 (3)	W(4)–Rh(4)	2.804 (2)
Rh(1)–Rh(2)	2.635 (3)	Rh(3)–Rh(4)	2.658 (3)
W(1)–P(1)	2.429 (8)	W(3)–P(5)	2.451 (6)
W(2)–P(2)	2.472 (8)	W(3)–P(6)	2.447 (7)
W(2)–P(3)	2.451 (6)	W(4)–P(7)	2.450 (7)
W(2)–P(4)	2.447 (7)	W(4)–P(8)	2.461 (8)
Rh(1)–P(1)	2.254 (7)	Rh(3)–P(5)	2.227 (7)
Rh(1)–P(2)	2.323 (8)	Rh(3)–P(6)	2.323 (8)
Rh(2)–P(3)	2.270 (7)	Rh(4)–P(7)	2.286 (8)
Rh(2)–P(4)	2.306 (7)	Rh(4)–P(8)	2.325 (7)
Rh(1)–Cc(1)	2.11 (2)	Rh(3)–Cc(3)	2.01 (3)
Rh(1)–Cc(2)	1.96 (2)	Rh(3)–Cc(4)	2.11 (2)
Rh(2)–Cc(1)	2.00 (3)	Rh(4)–Cc(3)	2.04 (2)
Rh(2)–Cc(2)	2.08 (2)	Rh(4)–Cc(4)	1.95 (2)
	(b) Angles (deg)		
W(1)–Rh(1)–Rh(2)	165.2 (1)	W(3)–Rh(3)–Rh(4)	167.7 (1)
Rh(1)–Rh(2)–W(2)	162.9 (1)	Rh(3)–Rh(4)–W(4)	165.0 (1)
W(1)–P(1)–Rh(1)	73.6 (2)	W(3)–P(5)–Rh(3)	73.9 (2)
W(1)–P(2)–Rh(1)	71.6 (2)	W(3)–P(6)–Rh(3)	72.4 (2)
W(2)–P(3)–Rh(2)	73.0 (2)	W(4)–P(7)–Rh(4)	72.5 (2)
W(2)–P(4)–Rh(2)	72.5 (2)	W(4)–P(8)–Rh(4)	71.7 (2)
Rh(1)–Cc(1)–Rh(2)	79.7 (8)	Rh(3)–Cc(3)–Rh(4)	81.9 (8)
Rh(1)–Cc(2)–Rh(2)	81.4 (8)	Rh(3)–Cc(4)–Rh(4)	81.7 (8)
Rh(1)–Cc(1)–O(1)	127 (2)	Rh(3)–Cc(3)–O(3)	148 (2)
Rh(1)–Cc(2)–O(2)	153 (2)	Rh(3)–Cc(4)–O(4)	126 (2)
Rh(2)–Cc(1)–O(1)	153 (2)	Rh(4)–Cc(3)–O(3)	130 (2)
Rh(2)–Cc(2)–O(2)	125 (2)	Rh(4)–Cc(4)–O(4)	152 (2)
P(1)–W(1)–P(2)	102.1 (3)	P(5)–W(3)–P(6)	102.3 (2)
P(3)–W(2)–P(4)	102.0 (2)	P(7)–W(4)–P(8)	102.9 (2)
P(1)–Rh(1)–P(2)	112.7 (3)	P(5)–Hrn3)–P(6)	111.4 (3)
P(3)–Rh(2)–P(4)	112.5 (3)	P(7)–Rh(3)–P(8)	112.8 (3)

summarized in Table II. A search for higher than triclinic symmetry was unsuccessful. A learned profile analysis was used to improve the accuracy of the measurement of weak reflections.

The structure was solved by automated Patterson projection interpretation methods[21] which readily located the four unique W positions. Subsequent difference Fourier syntheses located the remaining non-hydrogen atoms. A severely disordered, fractional occupancy molecule of CH_2Cl_2 was located and arbitrarily fixed at half occupancy. Refinement proceeded normally

(21) Sheldrick, G. SHELXTL (ver. 4.1) 1984, Nicolet Corp., Madison, WI.

Table VII. Interplanar Dihedral Angles and Torsion Angles for 13

plane	plane	interplanar angle (deg)
W(1)–Rh(1)–P(1)	W(1)–Rh(1)–P(2)	179.0 (1)
W(2)–Rh(2)–P(3)	W(2)–Rh(2)–P(4)	178.1 (1)
W(3)–Rh(3)–P(5)	W(3)–Rh(3)–P(6)	179.0 (1)
W(4)–Rh(4)–P(7)	W(4)–Rh(4)–P(8)	176.2 (1)
Rh(1)–Cc(1)–Rh(2)	Rh(1)–Cc(2)–Rh(2)	129.7 (3)
Rh(3)–Cc(3)–Rh(4)	Rh(3)–Cc(4)–Rh(4)	135.7 (3)

W(1)–Rh(1)–Rh(2)–W(2) = 147.1 (1)

W(3)–Rh(3)–Rh(4)–W(4) = −129.4 (1)

except for the high thermal parameters associated with the Cc(7)–O(7) and Cc(8)–O(8) carbonyl groups (unexpected) and the solvent molecule (expected). Due to the large number of atoms involved (245), only the W, Rh, P, and O atoms were anisotropically refined. Additionally, the phenyl rings were constrained as rigid bodies, and hydrogen atoms contributions were omitted. Atomic positional parameters are summarized in Table V, and selected bond distances and angles are given in Table VI.

X-ray Diffraction Study of 2. A deep red crystal of **2**, grown from pentane/CH_2Cl_2, was found to be isomorphous with its previously reported Ir analogue.[3] The details of data collection and refinement are provided in Table II. An empirical absorption correction was applied to the intensity data (max/min transmission = 1.21). Other aspects of the crystallographic work are as previously described.

The atomic coordinates from the Ir analogue provided a satisfactory initial model for this structure. The final refinement incorporated anisotropic temperature coefficients for all nonhydrogen atoms. The Rh-bound H atom was found and isotropically refined. As in the previous structure, the remaining H atoms were idealized (d(C–H) = 0.96 Å). Atomic coordinates are given in Table III and selected bond distances and angles in Table IV.

Acknowledgment. We thank the National Science Foundation (CHE 8201160) for support of this research and the Johnson-Matthey Co. for the loan of Rh salts.

Registry No. **2**, 88904-48-7; **3**, 105335-65-7; **4**, 105371-68-4; **7**, 105335-66-8; **8**, 105335-67-9; **9**, 88904-49-8; **10**, 105335-68-0; **13**, 105335-70-4; $[Rh(\mu\text{-}Cl)(COD)]_2$, 105335-64-6; $W(CO)_4(PPh_2H)_2$, 70505-43-0; *trans*-$RhCl(CO)(PPh_3)_2$, 15318-33-9; ethylene, 74-85-1.

Supplementary Material Available: Tables of anisotropic thermal parameters, calculated hydrogen atom positions, and complete bond lengths and angles, for **13** and **2** (11 pages); listings of observed and calculated structure factors for **13** and **2** (72 pages). Ordering information is given on any current masthead page.